Formation of Crystalline Nanoclusters of Ag, Cu, Os, Pd, Pt, Re, or Ru in a Silica Xerogel Matrix from Single-Source Molecular Precursors

Joseph P. Carpenter, C. M. Lukehart,* and Stephen B. Milne

Department of Chemistry, Vanderbilt University, Nashville, Tennessee 37235

D. O. Henderson and R. Mu

Physics Department, Fisk University, Nashville, Tennessee 37208

S. R. Stock

School of Materials Science and Engineering, Georgia Institute of Technology, Atlanta, Georgia 30332

Received July 3, 1997. Revised Manuscript Received October 7, 1997[⊗]

Metal complexes containing bifunctional ligands which possess alkoxysilyl functional groups have been prepared for seven metals of the first, second, or third transition metal series. Incorporation of these single-source precursors into silica xerogel matrixes using sol−gel chemistry affords molecularly doped xerogels. Subsequent thermal treatment of these doped xerogels under reducing or oxidizing-then-reducing conditions affords nanoclusters of Ag, Cu, Os, Pd, Pt, Re, or Ru which are highly dispersed throughout the bulk of the xerogel matrix. Characterization of these nanocomposite materials by TEM, EDS, XRD, and electron diffraction indicates that the metal nanoclusters are highly crystalline. A visible spectrum of the silver nanocomposite shows the expected surface plasmon resonance near 415 nm.

Introduction

Nanocomposite materials consisting of very small particles of a guest substance (typically having diameters less than 100 nm) dispersed throughout a host matrix are of intense current interest for potential applications in chemical catalysis or as magnetic, electronic, or photonic materials.[1−6] Materials containing metal nanoclusters have traditionally been prepared by a variety of chemical or physical methods including hydrosol formation, impregnation of a solid support, inert gas evaporation, vacuum evaporation, vacuum evaporation with cryogenic matrix isolation, cermet formation, pressure impregnation of a porous host, or cluster nucleation by irradiation.[7] Vast literature exists on the preparation of heterogeneous catalysts by the deposition or formation of metal particles on a solid support of high surface area.[8]

Recent interest in elemental metal clusters or colloids as chemical catalysts or in device fabrication has driven the development of other synthetic strategies.[2,8,9] Protected or passivated metal colloids have been prepared in which metal nanoparticles are coated with synthetic polymers, such as poly(vinyl alcohol), poly(methyl methacrylate), poly(vinyl pyrrolidone), polyimide films, or ROMP polymer blends;[10−13] cyclodextrins or cellulose derivatives;[14] surfactants; or surface-bound ligands, like thiols, phosphines, or water-soluble anions, such as OP-$(C_6H_4SO_3Na)_3$, *p*-$H_2N-C_6H_4SO_3Na$, or polyoxometalates.[15−18] Formation of metal particulates is effected in the presence of these passivating agents either through chemical reduction of metal ions in solution, as in the hydrosol method, or by using inorganic or organometallic molecules as single-source molecular precursors that decompose to give metal atoms. Reduction of metal ions also occurs within synthetic vesicles, micelles, phospholipid membranes, or polysilsesquioxanes.[19−21] Other reducing methods include use of glycol solvents, as in the polyol method,[22] use of alkalide and electride reagents,[23] or electrochemical reduction.[24]

* To whom correspondence should be addressed.

[⊗] Abstract published in *Advance ACS Abstracts,* November 15, 1997.

(1) Stucky, G. D. *Naval Res. Rev.* **1991**, *43*, 28.
(2) Sinfelt, J. H.; Meitzner, G. D. *Acc. Chem. Res* **1993**, *26*, 1.
(3) Steigerwald, M. L.; Brus, L. E. *Acc. Chem. Res* **1990**, *23*, 183.
(4) Wang, Y. *Acc. Chem. Res* **1991**, *24*, 133.
(5) Weller, H. *Angew. Chem., Int. Ed. Engl.* **1993**, *32*, 41.
(6) Weller, H. *Adv. Mater.* **1993**, *5*, 88.
(7) Halperin, W. P. *Rev. Mod. Phys.* **1986**, *58*, 533.
(8) Lewis, L. N. *Chem, Rev.* **1993**, *93*, 2693.
(9) Schmid, G. *Chem. Rev. (Washington, D.C.)* **1992**, *92*, 1709.
(10) Nakao, Y. *J. Chem. Soc., Chem. Commun.* **1993**, 826.
(11) Rubira, A. F.; Rancourt, J. D.; Caplan, M. L.; St. Clair, A. K.; Taylor, L. T.*Chem. Mater.* **1994**, *6*, 2351.
(12) Bradley, J. S.; Hill, E. W.; Behal, S.; Klein, C.; Chaudret, B.; Duteil, A.*Chem. Mater.* **1992**, *4*, 1234.
(13) Chan, Y. N. C.; Schrock, R. R. *Chem. Mater.* **1993**, *5*, 566.
(14) Duteil, A.; Chaudret, B.; Mazel, R.; Roucau, C.; Bradley, J. S. *Chem. Mater.* **1993**, *5*, 341.
(15) (a) Schmid, G.; Harms, M.; Malm, J.-O.; Bovin, J.-O.; van Ruitenbeck, J.; Zandbergen, H. W.; Fu, W. T. *J. Am. Chem. Soc.* **1993**, *115*, 2046. (b) Duteil, A.; Schmid, G.; Meyer-Zaika, W. *J. Chem. Soc., Chem. Commun.* **1995**, 31.
(16) Brust, M.; Walker, M.; Bethell, D.; Schiffrin, D. J.; Whyman, R. *J. Chem. Soc., Chem. Commun.* **1994**, 801.
(17) Amiens, C.; de Caro, D.; Chaudret, B.; Bradley, J. S.; Mazel, R.; Roucau, C. *J. Am. Chem. Soc.* **1993**, *115*, 11638.
(18) (a) Lin, Y.; Finke, R. G. *J. Am. Chem. Soc.* **1994**, *116*, 8335. (b) Aiken, J. D.; Lin, Y.; Finke, R. G. *J. Mol. Catal. Chem.* **1996**, *114*, 29.
(19) Choi, K. M.; Shea, K. J. *Chem. Mater.* **1993**, *5*, 1067.
(20) Lisiecki, I.; Bjorling, M.; Motte, L.; Ninham, B.; Pileni, M. P. *Langmuir* **1995**, *11*, 2385.
(21) Singh, A.; Markowitz, M. A.; Chow, G.-M. *Naval Res. Rev.* **1994**, *46*, No. 4, 17.

S0897-4756(97)00471-7 CCC: $14.00

Encapsulation of metal nanoclusters throughout the bulk of a porous ceramic matrix has been achieved using sol−gel procedures. Typically, metal salts or molecular precursors are added to sol−gel formulations prior to xerogel formation. Subsequent reduction of the metal ions or reductive decomposition of molecular precursors leads to the formation of metal nanoclusters throughout a xerogel matrix. Conventional metal oxide matrixes, such as silica or alumina xerogels, or hybrid inorganic−organic matrixes have been used as host materials.[25−28]

Schubert and co-workers examined the general scope of preparing metal nanoclusters in silica xerogel matrixes by the addition of metal salts to modified sol−gel formulations. For some metals, the observed metal particle size distributions are more narrow and monomodal when a bifunctional ligand molecule, such as $H_2NCH_2CH_2NH(CH_2)_3Si(OEt)_3$, is present in the sol−gel formulation. In situ complex formation presumably occurs between the dissolved metal ions and the diamine portion of the bifunctional ligand. Subsequent hydrolysis and condensation of the triethoxysilyl group of the bifunctional ligand during the sol−gel process leads to covalent incorporation of the metal complex into the silica xerogel matrix as it is being formed. Oxidative thermal treatment of the resulting xerogel affords metal oxide/xerogel composites, and subsequent reductive thermal treatment gives metal nanoclusters dispersed throughout the silica xerogel matrix. This procedure presumably results in a nearly homogeneous incorporation of metal ions within a silica xerogel matrix and affords metal nanoclusters with monomodal particle size distributions.[29−31]

We now report (1) the preparation of a wide variety of discrete mononuclear or polynuclear coordination complexes of low-valent metals containing bifunctional phosphine or thiolate ligands, (2) the incorporation of these complexes into a silica xerogel matrix as it is being formed, and (3) the formation of metal/silica xerogel nanocomposites following appropriate thermal treatment of these molecularly doped xerogels. The dopant complexes thus serve as preformed, single-source precursors to the resulting metal nanoclusters. In situ complexation of a metal ion by a bifunctional ligand is thereby obviated, and rapid dissociation of either phosphine or thiolate ligands from these precursors is not expected, as might be more likely with amine ligands. Metal/silica xerogel nanocomposites containing nanoclusters of Ag, Cu, Os, Pd, Pt, Re, or Ru are prepared using this strategy. Thermal conditions are chosen such that these metal nanoclusters are formed with sufficient size and crystallinity to permit characterization by diffraction methods. Such metal nanocomposites have potential application as heterogeneous catalysts or as nonlinear optical materials. An overview of metal/silica xerogel nanocomposite formation using this general synthetic strategy has been reported recently.[32]

Experimental Section

Reagents and Methods. The reagents tetramethyl orthosilicate (TMOS) and (3-mercaptopropyl)trimethoxysilane (HSR) were purchased from Aldrich Chemical Co., Inc. The thiol $HSCH_2SiMe(OEt)_2$ (HSR′) was purchased from Huls America, Inc. The reagent $Pt(COD)Cl_2$ [(η^4-1,5-cyclooctadiene)platinum-(II) chloride] was purchased from Strem Chemical Co., Inc. The bifunctional phosphines $Ph_2PCH_2CH_2Si(OCH_3)_3$ (L^A), $Ph_2PCH_2CH_2Si(OEt)_3$ (L^B), and $Et_2PCH_2CH_2Si(OEt)_3$ (L^C) were prepared according to literature procedures.[33] Reactions were performed in oven-dried glassware under a nitrogen or argon atmosphere. Tetrahydrofuran (THF), hexane, or ether were purified by distillation from sodium/benzophenone. Methylene chloride was dried by distillation from calcium hydride. Benzene was purified by distillation from sodium. Other solvents and reagents were used without further purification. Silica xerogels were formed at 25 °C using standard sol−gel formulations with minor modification of the procedure reported by Sakka.[34,35] All operations were performed at room temperature unless otherwise specified. Microanalyses were performed by Galbraith Laboratories, Inc., Knoxville, TN, or by Oneida Research Services, Inc., Whitesboro, NY. Samples containing osmium were not analyzed.

Proton, carbon, or phosphorus NMR spectra were recorded on a IBM NR-300 spectrometer operating at 300, 75, or 121 MHz, respectively, using the ^2H signal of the solvent as an internal lock frequency. Chemical shifts (in δ) were measured for ^1H NMR and ^{13}C NMR spectra relative to tetramethylsilane using the residual solvent peak as an internal standard, while chemical shifts (in δ) were measured for ^{31}P NMR spectra relative to an external standard of 85% H_3PO_4 with positive values being downfield of the respective references.

Nanocomposite materials were characterized by using a Philips CM20T transmission electron microscope (TEM) operating at 200 kV. Samples for TEM were prepared by dispersing a powdered sample of nanocomposite onto a 3-mm diameter copper grid covered with amorphous carbon as a substrate. These samples were analyzed with standard bright-field (BF) imaging for particle-size distribution, selected-area diffraction (SAD) for their crystal structures, and X-ray energy dispersive spectroscopy (EDS) for semiquantitative chemical composition.

X-ray diffraction (XRD) scans were obtained using a Philips PW1800 $\theta/2\theta$ automated powder diffractometer equipped with a Cu target and a postsample monochromator. Samples for XRD were prepared by placing a uniform layer of powdered nanocomposite onto double-sided tape affixed to the sample holder. The sample area was greater than the ca. 1 cm × 1 cm area irradiated by the X-ray beam. Considerable caution was used to keep the top of the sample surface flat and coplanar with the diffractometer rotation axis. Prior to peak width measurement, each diffraction peak was corrected for background scattering and was stripped of the $K\alpha_2$ portion of the diffracted intensity. The full-width-at-half-maximum (fwhm) was measured for each selected peak. Crystallite size, L, was calculated from Scherrer's equation, $L = K\lambda/(\beta \cos \theta_B)$, for peak broadening from size effects only (where β is the peak fwhm measured in radians on the 2θ scale, λ is the wavelength of X-rays used, θ_B is the Bragg angle for the measured hkl peak, and K is a constant equal to 1.00 for L taken as the

(22) (a) Kurihara, L. K.; Chow, G.-M.; Schoen, P. E. *Nanostructured Mater.* **1995**, *5*, 607. (b) Hirai, H.; Nakao, Y.; Toshima, N. *J. Macromol. Sci., Chem.* **1979**, *13*, 727.
(23) Tsai, K.-L.; Dye, J. L. *Chem. Mater.* **1993**, *5*, 540.
(24) (a) Reetz, M. T.; Helbig, W. *J. Am. Chem. Soc.* **1994**, *116*, 7401. (b) Reetz, M. T. in *Active Metals*, Furstner, A., Ed.; VCH: New York, 1996; Chapter 7.
(25) Nogami, M.; Abe, Y.; Nakamura, A. *J. Mater. Res.* **1995**, *10*, 2648.
(26) Kozuka, H.; Sakka, S. *Chem. Mater.* **1993**, *5*, 222.
(27) Tour, J. M.; Pendalwar, S. L.; Cooper, J. P. *Chem. Mater.* **1990**, *2*, 647.
(28) Choi, K. M.; Shea, K. J. *J. Am. Chem. Soc.* **1994**, *116*, 9052.
(29) Breitscheidel, B.; Zieder, J.; Schubert, U. *Chem. Mater.* **1991**, *3*, 559.
(30) Schubert, U. *New J. Chem.* **1994**, *18*, 1049.
(31) Morke, W.; Lamber, R.; Schubert, U.; Breitscheidel, B. *Chem. Mater.* **1994**, *6*, 1659.
(32) Carpenter, J. P.; Lukehart, C. M.; Milne, S. B.; Stock, S. R.; Wittig, J. E.; Jones, B. D.; Glosser, R.; Henderson, D. O.; Mu, R.; Shull, R. D.; Zhu, J. G.; Rek, Z. U. *SAMPE Technol. Conf.* **1995**, *27*, 549.
(33) Niebergall, H. *Makromol. Chem.* **1962**, *59*, 218.
(34) Brinker, C. J.; Scherer, G. W. *Sol−Gel Science*; Academic Press: New York, 1990.
(35) Adachi, T.; Sakka, S. *J. Mater. Sci.* **1987**, *22*, 4407.

volume-averaged crystallite dimension perpendicular to the *hkl* diffraction plane).[36a]

Optical spectra were recorded with a Hitachi 3501 double-beam spectrometer equipped with a 60-mm Hitachi integrating sphere fitted with a photomultiplier and a cooled PbS detector. Repeated measurements showed the photometric accuracy to be ±0.8% transmittance and ±0.7 nm in wavelength accuracy. Transmission measurements were made in the region between 240 and 1000 nm. The average particle size of the Ag nanoclusters (Si/Ag = 11:1) was determined from the line width of the surface plasmon absorption using the expression, $\Gamma = \tau^{-1} = 2\nu_f/d$, where Γ is the fwhm of the absorption band, τ is the Drude scattering time, ν_f is the Fermi velocity, and d is the particle diameter.[36b] This equation is based on a classical scattering model assuming spherical particles with the electron mean free path being entirely limited by boundary scattering.

Syntheses of Molecular Precursors 1a−7a. *Preparation of* $[AgSCH_2Si(Me)(OEt)_2]_7[AgCl]_3$, ***1a***. To a stirred suspension of silver(I) chloride (1.2 g, 8.1 mmol) in 20 mL of THF was added dropwise a solution of HSR′ (1.5 g, 8.1 mmol) in 20 mL of acetone. After this addition, triethylamine (0.81 g, 8.1 mmol) was added to the reaction suspension to give slow formation of a light yellow solution along with a white precipitate. After stirring for 24 h, the solvents were removed from the reaction suspension at reduced pressure to yield a yellow oil contaminated with triethylamine hydrochloride (based on ^{1}H NMR). The reaction residue was extracted with benzene. Removal of benzene from the extractant at reduced pressure gave 1.92 g (83.3% yield) of the product as a waxy yellow solid: ^{1}H NMR ($CDCl_3$) δ 0.37 (s, 3H, CH_3), 1.25 (t, $^3J_{HH}$ = 6.98 Hz, 6H, OCH$_2$CH_3), 2.23 (br s, 2H, CH_2), 3.84 (q, $^3J_{HH}$ = 6.98 Hz, 4H, OCH_2CH$_3$). Anal. Calcd for $[AgC_6H_{15}O_2SSi]_7[AgCl]_3$: C, 20.67; H, 4.34. Found: C, 20.47; H, 4.21. EDS analysis of both **1a** and a silica xerogel containing the molecular precursor **1b** revealed the presence of chlorine. Product **1a** is assumed to be a thiolate/chloride mixed-ligand polynuclear compound.

Preparation of Chlorotris(diphenyl[2-(triethoxysilyl)ethyl]-phosphine)copper(I), ***2a***. To a stirred solution of μ,μ'-dichlorobis[(η^4-1,5-cyclooctadiene)copper(I)][37] (0.22 g, 0.531 mmol) in 10 mL of benzene was added dropwise $Ph_2PCH_2CH_2Si(OCH_2CH_3)_3$ (1.20 g, 3.19 mmol). After 16 h, the solvent was concentrated at reduced pressure and pentane was added to the residue to induce crystallization. Cooling at −16 °C for 24 h afforded 1.41 g (72% yield) of the product as white needles: mp 120−122° C); ^{1}H NMR ($CDCl_3$) δ 0.65 (m, 2H, CH_2), 1.16 (t, $^3J_{HH}$ = 7.00 Hz, 9H, OCH$_2$CH_3), 2.17 (m, 2H, CH_2), 3.72 (q, $^3J_{HH}$ = 7.00 Hz, 6H, OCH_2CH$_3$), 7.25 (m, 4H, aromatic protons); ^{31}P{^{1}H} NMR ($CDCl_3$) δ −8.06 (s, phosphine). Anal. Calcd for $C_{60}H_{87}ClCuO_9P_3Si_3$: C, 58.65; H, 7.15. Found: C, 58.33; H, 7.32.

Preparation of $(\eta^6$-p-$MeC_6H_4CHMe_2)[Ph_2PCH_2CH_2Si(OCH_3)_3]$-$OsCl_2$, ***3a***. To a stirred solution of [(η^6-p-$MeC_6H_4CHMe_2$)-$OsCl_2]_2$ (0.300 g, 0.378 mmol),[38] where p-$MeC_6H_4CHMe_2$ is *p*-cymene, in 5 mL of methylene chloride was added a solution of $Ph_2PCH_2CH_2Si(OCH_3)_3$ (0.632 g, 1.89 mmol) in 15 mL of methylene chloride. After 2 h the reaction solution was evaporated to dryness at reduced pressure. The reaction residue was dissolved in 4 mL of methylene chloride and the addition of 20 mL of ether initiated precipitation of an orange solid. This mixture was stored at −30 °C for 24 h resulting in the formation of orange crystals which were isolated by filtration, washed with 4 × 5 mL of hexane, and dried at reduced pressure to give 0.443 g (80% yield) of the product as orange crystals: mp 184−186 °C; ^{1}H NMR ($CDCl_3$) δ 0.45 (m, 2H, PCH$_2$CH_2), 0.89 (d, 6H, CH(CH_3)$_2$), 2.00 (s, 3H, PhCH_3), 2.38 (sep, 1H, CH(CH$_3$)$_2$), 2.77 (m, 2H, PCH_2CH$_2$), 3.44 (s, 9H, OCH_3), 5.35 (m, 4H, C$_6H_4$), 7.45, 7.75−7.85 (m, 10H, P(C$_6H_5$); ^{31}P{^{1}H} NMR ($CDCl_3$) δ −15.9 (s, phosphine). Anal. Calcd for $C_{27}H_{37}Cl_2O_3OsPSi$: C, 44.44; H, 5.11. Found: C, 44.29; H, 5.24.

Preparation of Dibromobis(diethyl[2-(triethoxysilyl)ethyl]-phosphine)palladium (II), ***4a***. To a solution of (η^4-1,5-cyclooctadiene)palladium(II) bromide[39] (1.00 g, 2.67 mmol) in 20 mL of methylene chloride was added dropwise $Et_2PCH_2CH_2Si(OCH_2CH_3)_3$ (1.49 g, 5.43 mmol). After 24 h, the solvent was removed at reduced pressure, and the resulting solid was crystallized from methylene chloride/pentane solution at −20 °C to give 1.31 g (59% yield) of the product as yellow-orange crystals: mp 66−69 °C; ^{1}H NMR ($CDCl_3$) δ 0.82 (m, 2H, PCH$_2$CH_2Si), 1.12 (m, 6H, PCH$_2$CH_3), 1.24 (t, $^3J_{HH}$ = 6.98 Hz, 9H, OCH$_2$CH_3), 2.02 (m, 6H, PCH_2CH$_2$ and PCH_2CH$_3$), 3.84 (q, $^3J_{HH}$ = 6.98 Hz, 6H, OCH_2CH$_3$); ^{13}C{^{1}H} NMR ($CDCl_3$) δ 4.39 (s, SiCH$_2$), 8.27 (s, CH$_2$CH_3), 15.49 (m, PCH$_2$CH$_2$ & PCH$_2$-CH$_3$), 18.30 (s, OCH$_2$CH_3), 58.58 (s, OCH$_2$CH$_3$); ^{31}P{^{1}H} NMR ($CDCl_3$) δ 15.07 (s, cis phosphines, 90%), 16.85 (s, trans phosphines, 10%). Anal. Calcd for $C_{24}H_{58}Br_2O_6P_2PdSi_2$: C, 34.85; H, 7.08; P, 7.49. Found: C, 34.02; H, 6.69; P, 7.70.

Preparation of Dichlorobis(diphenyl[2-(trimethoxysilyl)ethyl]-phosphine)platinum (II), ***5a***. To a solution of (η^4-1,5-cyclooctadiene)platinum(II) chloride (1.00 g, 2.69 mmol) in 40 mL of methylene chloride was added dropwise a solution of $Ph_2PCH_2CH_2Si(OCH_3)_3$ (1.80 g, 5.38 mmol) in 5 mL of methylene chloride. The reaction solution became yellow but quickly faded to a clear, colorless solution. After 2 h, solvent was removed at reduced pressure to concentrate the reaction solution to 5 mL, and 50 mL of hexane was added to precipitate a white solid. The resulting mixture was stored at −30 °C for 16 h. The white precipitate was then isolated by filtration, washed with 3 × 10 mL of hexane, and dried at reduced pressure to give 2.19 g (87% yield) of the product. Recrystallization of this product from methylene chloride/hexane solution at −30 °C afforded white needles: mp 180−181 °C; ^{1}H NMR ($CDCl_3$) δ 0.80 (m, 4H, SiCH_2), 2.35 (m, 4H, PCH_2), 3.43 (s, 18H, OCH_3), 7.10−7.55 (m, 20H, PPh); ^{31}P{^{1}H} NMR ($CDCl_3$) δ 9.26 (s, 1, $^1J_{PtP}$ = 3662 Hz). Anal. Calcd for $C_{34}H_{46}Cl_2O_6P_2PtSi_2$: C, 43.68; H, 4.96. Found: C, 43.57; H, 5.10.

Preparation of Pentacarbonyl(diphenyl[2-(trimethoxysilyl)-ethyl]phosphine)rhenium Tetrafluoroborate, ***6a***. Following a reported procedure,[40] pentacarbonylmethylrhenium (0.413 g, 1.21 mmol) and triphenylcarbenium tetrafluoroborate (0.399 g, 1.21 mmol) were dissolved in 5 mL of methylene chloride and were allowed to react for 2 days, during which time a precipitate of pentacarbonyl(tetrafluoroborato)rhenium was formed. This precipitate was isolated by filtration, washed with 4 × 0.5 mL of methylene chloride, and was dried at reduced pressure to give 0.317 g (63.5% yield) of this intermediate as a white solid. To a suspension of pentacarbonyl-(tetrafluoroborato)rhenium (0.735 g, 0.178 mmol) in 8 mL of methylene chloride was added dropwise $Ph_2PCH_2CH_2Si(OCH_3)_3$ (0.059 g, 0.18 mmol). The reaction mixture was stirred for 24 h, and then the solvent was removed at reduced pressure, giving an off-white, waxy solid. Crystallization of this solid from methylene chloride/pentane solution at −30 °C gave 0.0771 g (58% yield) of the product as a waxy solid: mp 140 °C (dec); ^{1}H NMR ($CDCl_3$) δ 0.883 (m, 2H, SiCH_2), 1.27 (m, 2H, PCH_2), 3.54 (s, 9H, OCH_3), 7.57 (m, 10H, PPh); ^{31}P-{^{1}H} NMR ($CDCl_3$) δ −2.60 (s, m). Anal. Calcd for $C_{21}H_{23}BF_4O_7PReSi$: C, 35.35; H, 3.11. Found: C, 35.71; H, 2.85.

Preparation of Decacarbonyl-μ-hydrido-μ−(3-trimethoxysilyl)propanethiolato)-triangulo-triruthenium,[41] ***7a***. A solution of dodecacarbonyltriruthenium (0.31 g, 0.48 mmol) and HSR (0.094 g, 0.48 mmol) in 30 mL of benzene was refluxed for 15 min to give an orange suspension. This suspension was filtered, and the solvent was removed from the filtrate at reduced pressure to give an orange oil. Extraction of this oil with portions of hexane followed by removal of the hexane at reduced pressure gave the previously reported product[41] as an

(36) (a) Klug, H. P.; Alexander, L. E. *X-ray Diffraction Procedures for Polycrystalline and Amorphous Materials*, 2nd ed.; John Wiley & Sons: New York, 1974. (b) Halpwerin, W. P. *Rev. Mod. Phys.* **1986**, *58*, 533.

(37) Hende, J. H.; Baird, W. *J. Am. Chem. Soc.* **1963**, *85*, 1009.

(38) Cabeza, J. A.; Maitlis, P. M. *J. Chem. Soc., Dalton Trans.* **1985**, 573.

(39) Drew, D.; Doyle, J. R. *Inorg. Synth.* **1972**, *13*, 47.

(40) Beck, W.; Raab, K. *Inorg. Synth.* **1990**, *28*, 15.

(41) Evans, J.; Gracey, B. P. *J. Chem. Soc., Dalton Trans.* **1982**, 1123.

Table 1. Preparative Details and Analysis of Molecularly Doped Silica Xerogels

metal, sample no.	Ag, **1b**	Cu, **2b**	Os, **3b**	Pd, **4b**	Pt, **5b**	Re, **6b**	Ru, **7b**
precursor, μmol	**1a**, 14	**2a**, 85	**3a**, 69	**4a**, 90	**5a**, 40	**6a**, 103	**7a**, 645
TMOS (mmol)	1.35	0.85	3.39	4.5	4.0	1.03	6.45
mole ratio Si/M	101	13	50	52	100	11	3.7
water (mmol)	4.4	8.5	34.6	45	41	10.3	64.5
methanol (mL)	5	2		5		5	8
cosolvent	DMF	DMF	THF	DMF	THF	DMF	DMF
vol (mL)	(0.035)	(0.066)	(2.0)	(0.35)	(2.0)	(0.80)	(0.50)
catalyst[a]	basic	basic	acidic	basic	acidic	basic	basic
color	yellow	white	orange	yellow	yellow	white	orange
xerogel mass (mg)	170	160	263	632	367	188	1080
wt % of metal	0.95	2.05		1.29	1.76	6.36	9.86
wt % of Si	20.88	21.54		15.0	31.44	18.47	19.66
mole ratio Si/M	84	24		44	124	19	7

[a] Catalysts: acidic = 0.05 mL of 0.12 M aqueous HCl; basic = 0.02 mL of 0.148 M aqueous NH_3.

Table 2. Conditions for the Preparation of Metal/Silica Xerogel Nanocomposites

Metal, sample no.	Ag, **1c**	Cu, **2c**	Os, **3c**	Pd, **4c**	Pt, **5c**	Re, **6c**	Ru, **7c**
Precursor, mg	**1b**, 104	**2b**, 80	**3b**, 25	**4b**, 208	**5b**, 23	**6b**, 69	**7b**, 136
heat (air) *t*, *T* (°C)	1h, 600			2h, 700	2h, 500		
heat (H_2) *t*, *T* (°C)	5h, 600	3h, 600	0.5h, 900	1h, 700	2h, 500	2h, 700	3h, 700
final mass (mg)	83	36	20	83	18	37	94
color	red-brown	black	black	deep red	black	black	black
wt % of metal	1.37	4.28		2.34	2.66	10.92	(b)
wt % of Si	40.37	38.26		34.35	39.06	34.64	(b)
mole ratio Si/M	113	20		56	102	21	(b)
ave dia. (TEM, nm)	5.3	2.4	2.1	2.9	3.8	2.3	3.1
ave dia. (XRD, nm)	12.5	(a)	5.5	6.0	5.0	2.5	7.5

[a] XRD peaks too broad for accurate particle size measurement. [b] Low values of metal were determined due to precipitate formation.

orange oil: ^{1}H NMR ($CDCl_3$) δ −12.00 (s, 1H, hydride), 0.77 (m, 2H, CH_2CH_2Si), 1.79 (m, 2H, SCH_2CH_2), 2.18 (m, 2H, SCH_2CH_2), 3.57 (s, 9H, OCH_3); ^{13}C{H} NMR ($CDCl_3$) δ 8.39 (s, CH_2CH_2Si), 26.29 (s, SCH_2CH_2), 50.48 (s, OCH_3), 56.90 (s, SCH_2CH_2), 185.55 (s, *C*O), 191.71 (s, *C*O), 192.97 (s, *C*O), 198.19 (s, *C*O), 202.86 (s, *C*O), 204.34 (s, *C*O).

Syntheses of Molecularly Doped Silica Xerogels 1b−7b. Conventional sol−gel formulations were followed[34] for the synthesis of silica xerogels containing covalent incorporation of molecular precursors using modifications similar to those reported by Sakka.[35] Preparative details for each synthesis are shown in Table 1. All silica xerogels were formed at room temperature in plastic vials by hydrolysis of TMOS using either aqueous HCl or aqueous ammonia as catalyst. Molar ratios of total water to TMOS ranged from 4 to 10 with cosolvents being used to provide a solution of all reactants. Molar ratios of total silicon to molecular precursor ranged from 11 to 101. After addition of the specified catalyst, gels were aged at room temperature for 16−24 h. Wet xerogels were fractured, washed with methanol, and air-dried for several days or dried at reduced pressure for 30 min. Solvent washings from preparations using colored precursors indicated essentially complete incorporation of precursor molecules within the xerogel. Evaporated wash solutions did not produce detectable amounts of precursor residue.

Preparation of Metal/Silica Xerogel Nanocomposites 1c−7c from Molecularly Doped Silica Xerogels. The preparation of each metal/xerogel nanocomposite was performed using the same general procedure. A sample of a molecularly doped xerogel (prepared as described above) was ground to a powder and was then placed into an alumina boat (Fisher brand Combax). The alumina boat containing the sample was inserted into a quartz tube which was then placed into a Hoskins tube furnace. The atmosphere within the quartz tube was controlled by passing the desired gas through the tube at a rate of 150 mL per min, and the temperature of the sample was measured via an internal thermocouple placed directly above the sample. When the atmosphere around the sample was changed from air to hydrogen, nitrogen gas was passed through the tube for 15 min before the introduction of hydrogen gas was initiated. Temperature changes were ramped to the desired value at a rate of ca. 15°/min. Following thermal treatment, samples were cooled to room temperature over ca. 2 h.

Scheme 1

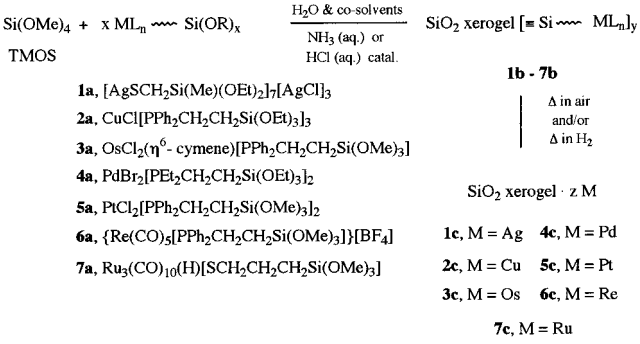

Specific procedures for the preparation of each nanocomposite are provided in Table 2. Oxidizing and reducing thermal treatments were used in the synthesis of nanocomposites **1c**, **4c**, and **5c**, while reducing conditions only were used to prepare nanocomposites **2c**, **3c**, **6c**, and **7c**. The thermal conditions reported gave metal nanoclusters of sufficient size and crystallinity to be characterized by diffraction methods. The metal nanocluster loading was high enough to produce deeply colored nanocomposites.

Results and Discussion

Metal/silica xerogel nanocomposites **1c−7c** have been prepared from molecular precursors (**1a−7a)** as shown in Scheme 1. These overall syntheses require three steps: (1) preparation of a single-source molecular precursor complex containing a bifunctional ligand, (2) covalent incorporation of these molecular precursors into a silica xerogel matrix as it is being formed, and, (3) a thermal treatment which transforms the molecularly doped xerogel host matrix into a metal/silica xerogel nanocomposite.

Molecular Precursors 1a−7a. Covalent incorporation of molecular precursors into a silica xerogel matrix as the matrix is being formed is accomplished by preparing molecular precursors which contain alkoxy-

silyl functional groups that can participate in sol−gel hydrolysis and condensation reactions. When metal complexes serve as molecular precursors, at least one ligand in the complex must be bifunctional, i.e., act as both a ligand to the metal atom and as a participant in the sol−gel chemistry of matrix formation. Molecular precursor complexes should also have adequate solubility properties and chemical stability to survive sol−gel conversion without chemical degradation.

The incorporation of bifunctional ligands into a molecular precursor is best accomplished as a final step in precursor synthesis. The product complex should be obtained in sufficiently high yield that it can be isolated by extraction and crystallization. Complex mixtures of products requiring chromatographic separations should be avoided because bifunctional ligands present in the desired complex can bond to conventional chromatographic supports. Synthetic strategies represented in the syntheses of precursors **1a**−**7a** are (1) partial exchange of chloride in AgCl by the sterically bulky thiolate, $^{-}SCH_2SiMe(OEt)_2$, to give a soluble complex, **1a**, (2) cleavage of metal−halide dimers by the phosphine L^B to give monomeric phosphine complexes **2a** and **3a**, (3) displacement of η^4-COD ligands by the bifunctional phosphines L^A, L^C, or L^B, affording complexes **2a**, **4a**, or **5a**, (4) displacement of a weakly coordinated tetrafluoroborato ligand by the phosphine L^A to give **6a**, and (5) formal oxidative addition of thiol HSR to $Ru_3(CO)_{12}$ to form **7a**.

Molecularly Doped Silica Xerogels 1b−7b. Silica xerogels containing covalent incorporation of each molecular precursor have been prepared using modified, though conventional, sol−gel formulations.[34,35] Details of these preparations are provided in Table 1. Choice of cosolvent is determined by the solubility properties of the precursor complex. Some nanocomposites have been prepared using different loading levels of molecular precursor or choice of catalyst from those conditions listed in Table 1; the dependence of nanocomposite properties on the variation of these reaction conditions is discussed below.

Covalent incorporation of precursors **1a**−**7a** into a silica xerogel matrix as it is being formed is supported by much previous work, as reported by Schubert,[29,30] Evans and Gracey,[41] and this laboratory.[42] EDS spectra of molecularly doped xerogels over multiple locations do not show significant variation in relative amounts of silicon or metal, thus indicating uniform incorporation of precursor on the micron scale. Furthermore, essentially all of the precursor complex at different loading levels is retained within the xerogel and cannot be extracted from the matrix by solvent washing. Control studies supporting this observation have been reported in a related system.[42]

Microanalytical data obtained on the air-dried xerogels **1b**−**7b** are difficult to interpret due, presumably, to various degrees of hydration/solvation of the xerogel matrix. More realistic determinations would require careful drying of these molecularly doped xerogels and storage under constant humidity. Microanalytical data obtained on the metal/silica xerogel nanocomposites following thermal treatment give more meaningful information (vide infra). In all cases, the ceramic yield of silica xerogel in **1b**−**7b** is at least 75%.

Metal/Silica Xerogel Nanocomposites 1c−7c. Metal/silica xerogel nanocomposites are prepared directly by thermal treatment of the molecularly doped xerogels **1b**−**7b**. Specific conditions for each thermal treatment are provided in Table 2. Thermal treatment under hydrogen as a final step affords metal nanoclusters of sufficient size and crystallinity to permit characterization by diffraction methods. The Ag, Pd, and Pt nanocomposites are prepared using both oxidizing and reducing thermal treatments, while the Cu, Os, Re, and Ru nanocomposites are obtained using only reducing thermal conditions. This latter observation demonstrates that low-valent complexes can degrade thermally to form metal nanoclusters without requiring explicit oxidation of ligand components. For the osmium and ruthenium nanocomposites, formation of the very volatile, and toxic, oxides OsO_4 or RuO_4 is thereby avoided.

Chemical microanalytical data for these nanocomposites reveal consistently high silicon content as expected for metal/SiO_2 compositions. Si/M molar ratios found for nanocomposites **1c** (Ag), **4c** (Pd), and **5c** (Pt) were within ca. 10% of those values used in the initial reaction stoichiometry, indicating a high retention of metal during the sol−gel synthesis and subsequent thermal treatment. Si/M molar ratios observed for nanocomposites **2c** (Cu) and **6c** (Re) indicate up to ca. 50% loss of metal in the overall synthesis. The mechanism by which this loss of metal occurs has not been studied.

The crystalline metal nanoclusters have been characterized by TEM, XRD, electron diffraction, and EDS. Representative TEM micrographs of each metal/silica xerogel nanocomposite are provided as Supporting Information, as are histograms of metal particle sizes. Metal nanoclusters are formed as nearly spheroidal particles with monomodal particle size distributions. Powder XRD scans for each nanocomposite (except for the Cu nanocomposite **2c**) are provided as Supporting Information, including patterns of the appropriate standard metal phases. The relatively small size of the Cu nanoclusters affords such broad XRD peaks that the XRD spectrum is essentially featureless. XRD diffraction data confirm the formation of crystalline metal particles. Selected-area electron diffraction data and EDS scans of each nanocomposite are also included as Supporting Information. From four to nine *d*-spacings expected for the appropriate crystalline metal are determined from the observed ring patterns. The absence of X-ray emissions from heavier elements, such as P, S, Cl, or Br, in the EDS spectra indicate that the thermal decomposition of the precursor complexes **1a**−**7a** is essentially complete.

Average values of metal particle diameters for these seven nanocomposites range from 2.1 to 5.3 nm by TEM and from 2.5 to 12.5 nm by XRD. Average particle diameters measured by TEM represent number-average values, whereas those values determined from XRD peak-width measurements are volume-weighted. Thus, the presence of a very small fraction of particles having diameters much larger than the number average value will give disproportionately larger average particle sizes by XRD. The close agreement of average metal particle

(42) Carpenter, J. P.; Lukehart, C. M.; Stock, S. R.; Wittig, J. E. *Chem. Mater.* **1995**, *7*, 201.

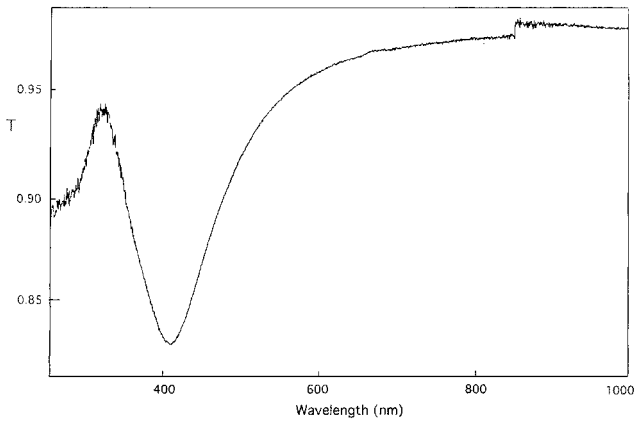

Figure 1. Optical transmission spectrum of the Ag/silica xerogel nanocomposite **1c**.

size by TEM and XRD for nanocomposite **6c** indicates that very few exceptionally large particles of Re are present in the sample.

Other observations worthy of note include the following.

(1) Silver nanocomposite prepared using a Si/Ag stoichiometry of 11/1 (nearly a 10-fold increase in precursor loading) gives only a 25% increase in the average size of the Ag nanoparticles (6.6 nm by TEM and 17.5 nm by XRD). However, the formation of a small fraction of unusually large Ag particles is apparent from the XRD data.

(2) The optical transmission spectrum of the Ag nanocomposite **1c** was recorded using a powdered sample and an integrating-sphere spectrometer. This spectrum, shown in Figure 1, shows the expected surface plasmon absorption at 415 nm. On the basis of Mie theory, Creighton and Eadon calculate that 10 nm Ag particles in a dielectric medium with a refractive index equal to that of water should exhibit a surface plasmon resonance slightly below 400 nm.[43] Using multitarget sputtering, Tanahashi and co-workers prepared silver nanoclusters in SiO_2 glass.[44] Surface plasmon resonances for these silver particles having average diameters of 10.5, 15.3, or 18.7 nm appear at ca. 410 nm, a resonate frequency very close to that observed for Ag/silica xerogel nanocomposite **1c**, as expected due to the similarity of the host matrixes. Silver nanoclusters supported in other solid host matrixes give surface plasmon maxima from 440 to 458 nm.[45−47] Line width measurements of the surface plasmon resonance for the silver/silica xerogel nanocomposite prepared using a Si/Ag stoichiometry of 11/1 give a calculated average silver particle size of 14 nm.[36b] This value is in reasonable agreement with that determined by XRD (17.5 nm).

(3) Use of either aqueous HCl or NH_3 as sol−gel catalyst gives no significant change in particle size distribution for the Os nanocomposite. However, identical samples of doped xerogel **3b** when treated under hydrogen for either 2 h at 500 °C or for 4 h at 700 °C give osmium particle size distributions of 1−5 nm or 2−9 nm, respectively. Growth in metal particle size within a host matrix upon prolonged thermal treatment is expected for coalescence processes controlled by mass diffusion.[44]

(4) The known complex $Os_3(CO)_{10}(\mu\text{-H})[\mu\text{-S}(CH_2)_3Si(OMe)_3]$[41] was also used as a molecular precursor of osmium/silica xerogel nanocomposites using the above sol−gel synthetic method. In all cases, the Os nanoclusters had noticeably nonspherical shapes;[48] however, the origin of this effect was not investigated.

(5) A 5-fold increase in the loading level of **4a** in the molecularly doped silica xerogel followed by the same thermal treatment gives a Pd/silica xerogel nanocomposite containing a bimodal particle-size distribution of Pd nanoclusters. These Pd particulates range in size from 1.7 to 13.9 nm and have an average diameter of 5.9 nm.

(6) Preparaton of the Pt nanocomposite using either increased precursor loading (50/1) or higher temperatures for the thermal treatments (700 °C) gives essentially no change in Pt nanocluster size distribution. However, Pt nanocluster size distributions differ for use of either acidic (0.07 mL, 0.12 M HCl; 3.3 nm average diameter, 1−6 nm range) or basic (0.05 mL, 0.148 M NH_3; 5.9 nm average diameter, 1−12 nm range) catalysts for the sol−gel conversion. Hydrolysis rates of tetraalkyl orthosilicates and organotrialkoxysilanes, $RSi(OR)_3$, are much more similar under acid catalysis than under base catalysis.[34,49] Therefore, cohydrolysis of TMOS and precursors such as **5a** under acid catalysis might afford a more homogeneous doping of the resultant xerogels. Also, acid-catalyzed xerogels tend to form more linear intrinsic silica strands having a small average pore size while xerogels prepared using a basic catalyst form more branched intrinsic structures having larger average pore sizes.[34] One might expect smaller Pt nanocluster formation from acid-catalyzed silica xerogels as Pt atoms or polyatomic clusters migrate throughout a more uniformly doped matrix into the pores of the xerogel where nanocluster formation occurs.

Other synthetic routes to metal particulates of the metals reported herein are available.[50−59]

Conclusions

A general synthetic strategy for the preparation of metal/silica xerogel nanocomposites has been demon-

(43) Creighton, J. A.; Eadon, D. G. *J. Chem. Soc., Faraday Trans.* **1991**, *87*, 3881.
(44) Tanahashi, I.; Yoshida, M.; Manabe, Y.; Tohda, T. *J. Mater. Res.* **1995**, *10*, 362.
(45) Arai, M.; Mitsui, M.; Ozaki, J.; Nishiyama, Y. *J. Colloid Interface Sci.* **1994**, *168*, 473.
(46) White, C. W.; Thomas, D. K.; Hensley, D. K.; Zuhr, R. A.; McCallum, J. C.; Pogany, A.; Haglund, R. F.; Magruder, R. H. *Nanostruct. Mater.* **1993**, *3*, 447.
(47) Kreibig, U.; Genzel, L. *Surface Sci.* **1985**, *156*, 678.
(48) Ahmadi, T. S.; Wang, Z. L.; Green, T. C.; Henglein, A.; El-Sayed, M. A. *Science* **1996**, *272*, 1924.
(49) Hench, L. L.; West, J. K. *Chem. Rev. (Washington, D.C.)* **1990**, *90*, 33.
(50) Li, X.; Vannice, A. *J. Catal.* **1995**, *151*, 87.
(51) Roy, B.; Roy, S.; Chakravorty, D. *J. Mater. Res.* **1994**, *9*, 2677.
(52) De, G.; Epifani, M.; Licciulli, A. *J. Non-Cryst. Solids* **1996**, *201*, 250.
(53) Terry, K. W.; Lugmair, C. G.; Gantzel, P. K.; Tilley, T. D. *Chem. Mater.* **1996**, *8*, 274.
(54) Schubert, U.; Tewinkel, S.; Lamber, R. *Chem. Mater.* **1996**, *8*, 2047.
(55) Bonnemann, H.; Brijoux, W.; Joussen, T. *Angew. Chem., Int. Ed. Engl.* **1990**, *29*, 273.
(56) Lewis, L. N.; Lewis, N. *Chem. Mater.* **1989**, *1*, 106.
(57) Psaro, R.; Dossi, C.; Fisco, A.; Ugo, R. *Res. Chem. Intermed.* **1991**, *15*, 31.
(58) Mizushima, T.; Tohji, K.; Udagawa, Y.; Ueno, A. *J. Am. Chem. Soc.* **1990**, *112*, 7887.
(59) Yingjie, Z.; Yitai, Q.; Hai, H.; Manwei, Z.; Li, Y. *J. Mater. Sci. Lett.* **1996**, *15*, 1346.

strated. Relatively simple metal phosphine and thiolate complexes or more complex metal carbonyl, η^6-arene, and cluster complexes survive sol−gel reaction conditions and serve as preformed, single-source molecular precursors to a desired metal nanocluster. The presence of bifunctional ligands in the molecular precursors ensures covalent and homogeneous incorporation of these complexes within the silica xerogel matrix as it is being formed. Within the solubility limits of the molecular precursor, variation of the TMOS/precursor stoichiometry permits variation of the metal weight percent in the resulting nanocomposite.

Seven metal/silica xerogel bulk nanocomposites have been prepared including representative metals from the first, second, and third transition metal series. Crystalline metal nanoclusters having average diameters of 2.1−5.3 nm (by TEM) and monomodal particle-size distributions are obtained following thermal treatment of silica xerogels doped with the appropriate molecular precursor. When low-valent metal complexes are used as precursors, metal nanoclusters (such as those of Ru or Os) can be formed by direct reductive thermal treatment, thereby avoiding the formation of volatile metal oxide intermediates. Extension of this synthetic strategy to the preparation of other silica xerogel nanocomposites appears promising, particularly for binary element/silica xerogel nanocomposites where the stoichiometry of the binary nanocluster substance is controlled by the chemical composition of the preformed molecular precursor. Results of such studies will be reported in future publications.

Acknowledgment. C.M.L. thanks the donors of the Petroleum Research Fund, administered by the American Chemical Society, for partial support of this research and to support by, or in part by, the U.S. Army Research Office under grant number DAAH04-95-1-0146. Work performed at Fisk University was supported by NASA under Grant No. NAG8-1066 (D.O.H.) We thank Dr. James E. Wittig for assistance in managing the TEM Facility within the Department of Applied and Engineering Sciences at Vanderbilt University and Mr. Scott Lowrie for assistance in acquiring powder XRD data at the Georgia Institute of Technology.

Supporting Information Available: TEM micrographs, histograms of metal nanocluster particle-size distributions, powder XRD pattersns, selected-area electron diffraction data, and EDS spectra for all metal/silica xerogel nanocomposites (17 pages). Ordering information is given on any current masthead page.

CM970471T